A Fast SPAD-Based Small Animal Imager for Early-Photon Diffuse Optical Tomography

Ying Mu and Mark Niedre, *IEEE Member*

Abstract— **Photon scatter is the dominant light transport process in biological tissue and is well understood to degrade imaging performance in near-infrared diffuse optical tomography. Measurement of photons arriving at early times following a short laser pulse is considered to be an effective method to improve this limitation, i.e. by systematically selecting photons that have experienced fewer scattering events. Previously, we tested the performance of single photon avalanche photodiode (SPAD) in measurement of early transmitted photons through diffusive media and showed that it outperformed photo-multiplier tube (PMT) systems in similar configurations, principally due to its faster temporal response. In this paper, we extended this work and developed a fast SPAD-based time-resolved diffuse optical tomography system. As a first validation of the instrument, we scanned an optical phantom with multiple absorbing inclusions and measured full time-resolved data at 3240 scan points per axial slice. We performed image reconstruction with very early-arriving photon data and showed significant improvements compared to time-integrated data. Extension of this work to mice *in vivo* and measurement of time-resolved fluorescence data is the subject of ongoing research.**

I. Introduction

Near-infrared (NIR) light in the wavelength range from 680 to 1000 nm can penetrate several centimeters into biological tissue, although light transport is dominated by scattering. Diffuse optical tomography (DOT) utilizes multi-projection measurements and physical models of photon propagation and retrieves the distribution of intrinsic optical properties (μ_s and μ_a) or fluorophores in biological tissues. However, the high degree of photon scattering is a persistent problem and leads to a highly ill-posed inverse problem that reduces the imaging resolution in DOT and diffuse fluorescence tomography (DFT) [1]. Time-resolved (TR) measurement of early-transmitted photons from an ultrafast laser source has been studied as a method for improving this limitation by a number of groups including ours [2-5]. The concept is that the photons arriving earliest at a detector from a pulsed laser have experienced fewer average scattering events and have taken relatively less diffuse paths. In practice, this has been shown to reduce the width of "photon density sensitivity function" (PDSF or Jacobian) between a source-detector pair, resulting in a better conditioned inverse problem and improved imaging resolution.

In recent years, our group has performed a series of studies to characterize the "early photon effect" in detail. Among other instrument properties, we studied the dependence of the relative reduction in PDSF width (versus ungated-CW photons) on the instrument temporal impulse response function (TIRF) [6]. We showed that faster combinations of detectors and electronics (instruments with lower TIRFs) provided better EP performance relative to theoretical maximum predicted by Monte Carlo (MC) models of photon transport. Recently we tested a fast single photon avalanche photodiode (SPAD; ID-100-50; ID Quantique, Geneva, Switzerland) with a TIRF in the range of 30-40 ps. We showed that the SPAD was effective in measuring EPs through tissue-mimicking optical phantoms and yielded the narrowest PDSFs that we have been able to achieve. These were approximately 65% narrower than the un-gated case, exceeding the performance of photomultiplier tube (PMT) systems and approaching the theoretical maximum predicted by time-resolved MC simulations [7].

It is well known that PDSF width is directly correlated to DOT imaging resolution. Therefore, we next developed a SPAD-based time-resolved small animal DOT imaging system. In this work, we describe this instrument and show initial results in tissue-simulating optical phantoms with multiple attenuating target inhomogeneities. This system allowed us to acquire full-time transmitted photon measurements with approximately 50 ps temporal resolution. We performed 360^o multi-projection scanning and generated tomographic axial reconstructions with early-time and quasi-CW data. As we show, the improvements in imaging performance are significant, and show the potential for our SPAD-based system to further improve resolution in diffuse photon imaging. Ongoing work includes application of this scanner in fluorescence imaging and in mice *in vivo*.

II. Method and Materials

A. Experimental setup

A schematic and photograph of the SPAD-based time-resolved scanner is shown in Figure 1. We used a femtosecond Titanium:Sapphire laser (MaiTai XF-1, Newport Corporation, Irivine ,CA) operating at 750nm and fitted with a variable attenuator (VA), so that the incident power at the sample was adjustable. The sample was mounted on a smaller rotatable stage controlled by stepper motor (VELMEX Inc). The transmitted light from the sample was measured by three

Research supported by NIH Foundation.

Ying Mu is a Graduate student, Department of Electrical and computer Engineering, Northeastern University, Boston, MA, 02115, USA (e-mail: mu.y@ husky.neu.edu).

Mark Niedre is an assistant professor, Department of Electrical and computer Engineering, Northeastern University, Boston, MA, 02115, USA (e-mail: mniedre@ ece.neu.edu).

SPAD detectors, which were mounted on a larger rotatable stage. The spacing angle between them was 35°. The outer stage could be rotated – in this case to 3 angular positions – so that the object could be scanned many source-and-detector combinations. The SPADs were connected to a router (HRT-82; Becker&Hickl, Berlin, Germany) which could be incorporated with a time correlated single photon counting module (SPC-130; Becker&Hickl) to perform parallel acquisition of time-resolved signals on all 3 channels simultaneously. The measurement was synchronized to the laser pulse using an optical constant fraction discriminator (OCFD). The electronic temporal resolution was about 6 ps, with an overall instrument TIRF FWHM of 50 ps as shown in fig. 1c.

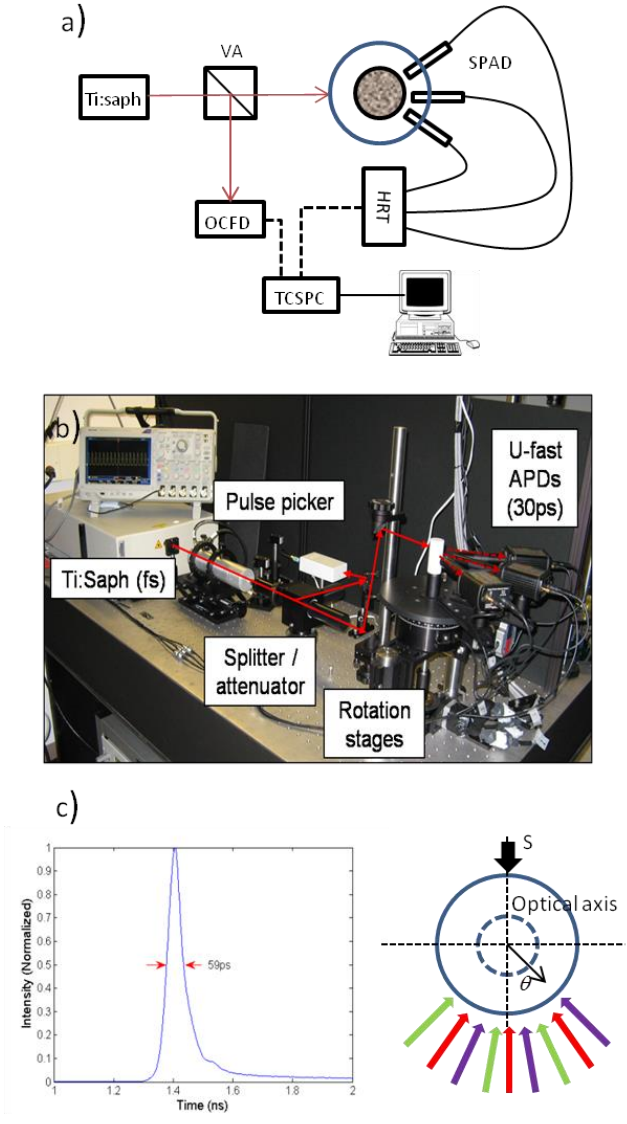

Figure 1. a) Schematic and (b) photograph of the SPAD-based DOT imager. The path of the excitation light and the detection geometry is. (c) Overall measured system TIRF showing the fast instrument response. (d) Diagram showing the 9-detector positions, achieved by rotating the outer stage in 3 positions (shown in green, red and purple).

B. *Optical phantom and data collection*

In order to characterize the performance of our instrument we developed a custom optical phantom as shown in fig. 2. A 25mm diameter x 100 mm long resin cylindrical phantom was machined into a hollow container with inner diameter of 22 mm. Twelve, 2 mm diameter holes were drilled at different positions in the solid bottom. Absorbing rods could then be in inserted into specific holes (or combinations of holes) and the phantom was filled with matching liquid phantom (1% Intralipid, 50 ppm ink, with optical properties approximately equal to $\mu'_s = 15\ cm^{-1}$ and $\mu_a = 0.1cm^{-1}$). In this way, we could flexibly select the position and number of absorption inclusions for characterization of our instrument and image reconstruction algorithm.

During acquisition, the phantom was rotated over 360° with 1° increments. After full rotation of the inner stage the outer motor stage was moved by ±10°, positioning the detectors at ±45°, ±35° , ±25° , ±10° and 0° angles from the optical axis. Thus, 3240 measurements were sampled for each axial slice.

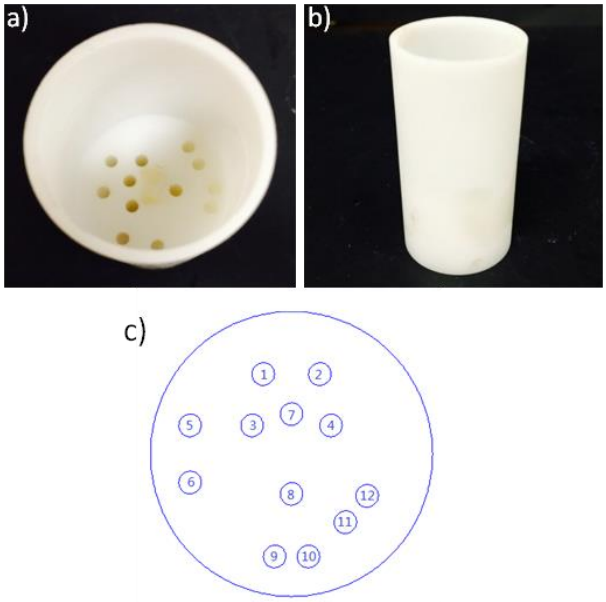

Figure 2. Photos of the fabricated optical phantom:a) Top view and b) Side view c) diagram showing disytibution and number of holes

C. *Tomographic Image Reconstruction Strategy*

Generally, forward modeling in diffuse optical tomography is performed using an approximation to the Boltzmann Transport Equations (BTE) or with Monte Carlo (MC) simulations. In the case of imaging with "quasi-CW" (i.e. time-integrated) photons, the time-independent diffusion approximation is frequently used and is generally considered to yield acceptable accuracy in small animal imaging geometries. In this case, the "weight matrix" W between a source and detector pair for the linearized image reconstruction problem is given by:

$$W(r_s, r_d) = \int U_0(r, r_s) G(r_d, r) dr^3 \qquad (1)$$

in which, r_s *and* r_d are the locations of the source and detector, respectively and r is a coordinate within the diffusive medium. U_0 and G can be calculated by the solution of diffusion equation for a point source in an infinite medium:

$$\Phi(r) = \frac{1}{4\pi D r} \exp\left(-\sqrt{\frac{\mu_a}{D}} r \right) \qquad (2)$$

where Φ is the photon fluence rate and $D = [3(\mu'_s+\mu_a)]^{-1}$.

Modeling of time-dependent photon propagation at early times is a complicated problem and is still a subject of debate in the field. Time-resolved Monte Carlo (MC) simulations have been used previously (e.g. [8]) since MC is a direct numerical implementation of the BTE. However, time-resolved MC methods are computationally very expensive (particularly at very early time points were few photons are detected) and may require long simulation times (on the order of hours) even on modern computers with hardware acceleration.

We and others have also used the time-dependent diffusion approximation to the BTE. Here, the time-resolved weight matrix W is given by:

$$W(r_s, r_d, t) = \int \int_0^t U_0(r, r_s, \tau) G(r_d, r, t-\tau) d\tau dr^3 \qquad (3)$$

, and the time-resolved solution to the diffusion equation for a point source in an infinite medium is given by:

$$\Phi(r,t) = \frac{c}{(4\pi D c t)^{3/2}} \exp\left(-\frac{r^2}{4Dct} - \mu_a c t \right) \qquad (4)$$

Although the diffusion approximation is widely considered to be less accurate than MC methods (particularly for early time points following a short laser pulse) this method is extremely computationally efficient. Moreover, our experimental analysis indicates that Weight functions computed with diffusion theory provide very good agreement with MC solutions except at extremely early (<1% on the rising edge of the transmitted time-resolved curve) in for the geometries considered here (publication in preparation). Therefore, we chose to compute W using the TR diffusion approximation.

We used a linear image reconstruction strategy [9], where the forward problem is posed as a system of equations: $[y]=[W][\delta\mu_a]$ where y is the set of source-detector pair measurements, W is the corresponding "weight matrix" and $\delta\mu_a$ is the absorption due to the inclusions. The inverse problem was solved using the commonly used randomized algebraic reconstruction technique (r-ART). The number of iterations and regularization parameter use were identical in all cases.

For each time-resolved measurement (figure 3a) we analyzed two data types: an early-time gate and quasi-CW (time-integrated) data. (However, joint use of the entire full-time curve in image reconstruction is the subject of ongoing work). For early-time case, we summed data in a 120 ps window centered at approximately 25% of the peak on the rising edge of the time-resolved transmission curve. For quasi-CW case data was summed over all time bins in the time-resolved curve..

III. Results

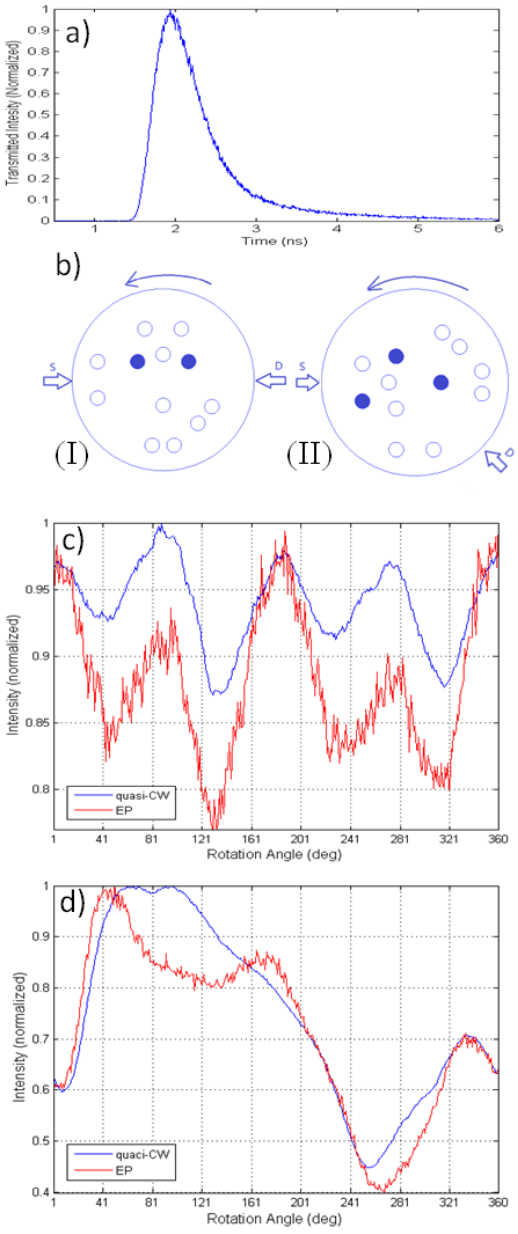

Figure 3. a) Measured time-resolved normalized transmitted photon density b) Two example absorber configurations. Normalized measured data are shown as a function of rotation angle for early time points and quasi-CW data. c) Detector at 0 deg away from the optical axis for configuration-I. d)Detector at -45 deg away from the optical axis for configuration-II

A. Measured Data

We tested a number of combinations of absorbers with our phantom, and two example configurations are shown in figures 3 and 4: (I) 2 absorbing rods inserted at a relatively deep position, 10mm away from the surface with a center-to-center separation of 7 mm; (II) Three absorbing rods

inserted at positions corresponding to different depths. Example normalized quasi-CW and EP data types as a function of rotation angles for the two phantom configurations are shown in figures 3b and c. For the first phantom (I) data from the detector aligned with the optical axis (0^o) are shown. For phantom (II), data are shown for the detector offset -45^o optical axis. (Similar curves were generated for each source detector and pair combination). For both phantoms, the EP data shows more structure due to the absorber attenuation than the quasi-CW case, e.g. a "dip" around 100^o rotation angle of EP trace in case (II) , which could not been seen with the quasi-CW curve. Although difficult to interpret directly, our simulations confirm that this structures relates to the target separation (not shown for brevity) and directly leads to better reconstruction in the inverse problem.

B. *Axial reconstructed images*

Fig.4 shows the reconstructed images for the two example phantom configurations presented in cases (I) and (II). The "correct" positions are shown in figs 4a and d. Figs. 4b,e are reconstructed by using quasi-CW data and steady state weight matrix derived by Eqns. 1 and 2. Figs. 4c,f are the reconstructions obtained from the EP data data type and weight matrix. The green circles in each image label the true

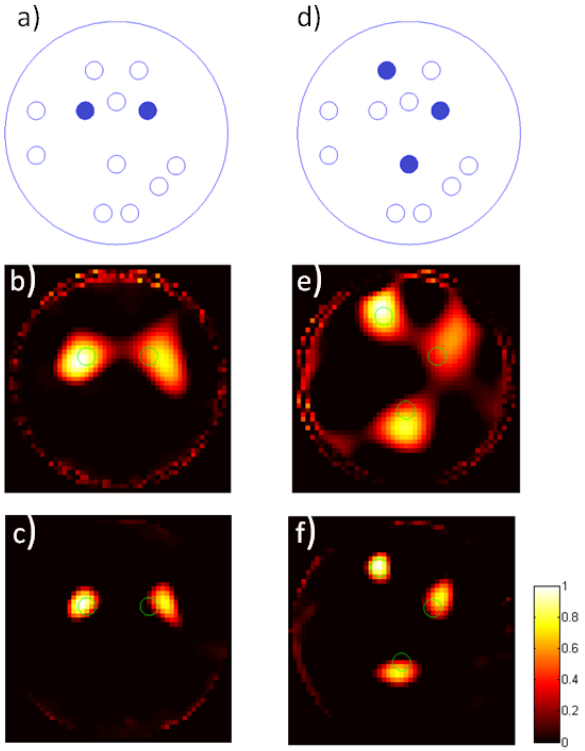

Figure 4. Reconstructed images: (a,d) absorber positions. (b,e) Reconstruction with quasi-CW data and steady state weight matrix. (e,f) Reconstruction with EP data and TR weight matrix.

location and size of the absorption heterogeneities for comparison. By inspection it is clear that the EP data type yields significantly better performance in image domain. Though the number and approximate position of the targets could also be retrieved with the quasi-CW data, significantly worse resolution, positioning and separation are evident. The differences were more marked when 3 absorbing inclusions were used in the phantoms and when absorbers were included at deeper positions. Reconstructions performed with EP data showed marked improvement with excellent localization and separation between the targets.

IV. Conclusion

In summary, we constructed a novel SPAD-based time-resolved DOT system with extremely fast temporal response. We validated this instrument with a custom fabricated optical phantom that allowed testing of multiple combinations of target absorber configurations. Our preliminary data clearly demonstrates the improvement in imaging domain obtained with this design when early-photons were measured. Full characterization of the imaging performance of this system is ongoing. We next plan to apply the imaging system to small animals and evaluate its performance under more complex optical environments[10] .Finally, we are developing a similar configuration for fluorescence imaging.

Acknowledgment

This work was funded with a grant from the National Institute of Health (R01EB012117).

References

[1] Arridge, Simon R. "Optical tomography in medical imaging." *Inverse problems* 15, no. 2 (1999): R41.

[2] Hebden, Jeremy C., Simon R. Arridge, and David T. Delpy. "Optical imaging in medicine: I. Experimental techniques." *Physics in medicine and biology* 42, no. 5 (1997): 825.

[3] Kneipp, Katrin, Yang Wang, Harald Kneipp, Lev T. Perelman, Irving Itzkan, Ramachandra R. Dasari, and Michael S. Feld. "Single molecule detection using surface-enhanced Raman scattering (SERS)." *Physical review letters* 78, no. 9 (1997): 1667.

[4] Venugopal, Vivek, Jin Chen, and Xavier Intes. "Development of an optical imaging platform for functional imaging of small animals using wide-field excitation." *Biomedical optics express* 1, no. 1 (2010): 143.

[5] Li, Zhi, and Mark Niedre. "Hybrid use of early and quasi-continuous wave photons in time-domain tomographic imaging for improved resolution and quantitative accuracy." *Biomedical optics express* 2, no. 3 (2011): 665-679.

[6] Valim, Niksa, James Brock, Miriam Leeser, and Mark Niedre. "The effect of temporal impulse response on experimental reduction of photon scatter in time-resolved diffuse optical tomography." *Physics in medicine and biology* 58, no. 2 (2013): 335.

[7] Mu, Ying, Niksa Valim, and Mark Niedre. "Evaluation of a fast single-photon avalanche photodiode for measurement of early transmitted photons through diffusive media." *Optics letters* 38, no. 12 (2013): 2098-2100.

[8] Chen, Jin, Vivek Venugopal, and Xavier Intes. "Monte Carlo based method for fluorescence tomographic imaging with lifetime multiplexing using time gates." *Biomedical optics express* 2, no. 4 (2011): 871-886.

[9] Wang, Lihong V., and Hsin-I. Wu. *Biomedical optics: principles and imaging*. John Wiley & Sons, 2012.

[10] Niedre, Mark, and Vasilis Ntziachristos. "Comparison of fluorescence tomographic imaging in mice with early-arriving and quasi-continuous-wave photons." *Optics letters* 35, no. 3 (2010): 369-371.